3D Generalized Langevin Equation (GLE) Approach to Gas-Surface Energy Transfer : Model H + H → H_2/Si(100)-(2×1)

Youxiang Zhang and Seung Chul Park*

Department of Chemistry and Institute of Basic Science, Sungkyunkwan University, Suwon 440-746, Korea
Received August 16, 2000

we have proposed a three-dimensional GLE approach to gas-surface reactive scattering, model H + H → H_2/Si(100)-(2 × 1) system, and the implementation of 3D GLE method on the hydrogen on silicon surface has been presented. The formalism and algorithm of the 3D GLE are worked properly in the reactive scattering system. The calculated normal mode frequencies of surface vibrations were almost identical to previous harmonic slab calculations. The reaction probabilities were calculated for two energies. The calculations show that a very large amount of energy is transferred in surface in low energy scattering. Three different types of reaction mechanisms has been observed, which can not be shown in flat and rigid surface models. Further work on the reaction mechanisms and calculations of the vibrational and rotation distributions of products is in progress. The results will be reported elsewhere soon.

Introduction

The dynamics of energy transfer, bond dissociation, and bond formation in gas-surface interaction systems are of fundamental importance[1-3] not only in basic science but also in many industrial processes such as heterogeneous catalysis and microelectronics fabrication. The process of energy transfer through translation to internal vibrations and/or vibrations to surface vibrations is a prerequisite to subsequent surface-assisted bond dissociation steps. Therefore, elucidation of the extent and nature of energy transfer to adsorbed molecules, including the dynamics of adsorbed molecule-surface bond motion, represents a problem essential to surface reactions. In recent years, scientists in the field of gas-surface interactions have made impressive progress, producing many important results.[4-20] Among the solid surfaces, silicon surfaces have attracted extensive attention in recent years.[14-20] The main reason for that is silicon surfaces are widely used in the micro-fabrications of VSLI circuits.[3]

In the early stages of research, the gas-surface energy transfer on silicon surfaces was studied in the inelastic scattering between gas atoms to vibrational motion of finite slab of silicon surfaces.[17-19] Lucchese and Tully[20] have reported surface rainbow scattering of He-Si(100) on reconstructed and unreconstructed surfaces and have shown the importance of the structure of the surfaces. Park and Bowman[17-19] have reported phonon inelastic scattering of He atoms on a silicon surface using the DECENT method[5,6] They calculated the energy transfer into each phonon mode and the transition probabilities by quantum mechanical method using a harmonic lattice. After the Eley-Rideal(ER) mechanism was observed for a variety of hydrogen-induced exothermic reactions on metal surfaces,[4,5] theoretical studies shifted to reactive scattering on metal and silicon surfaces.[13-15] Jackson and Persson[21-24] have reported the time-dependent wavepackets calculations of recombinative desorption of atomic hydrogen on a copper surface, first with a two-dimensional collinear model[21,22] and later with a fully three-dimensional flat surface model for Cu surface.[23] The effects of isotopic substitution on ER reactions and adsorbate-mediated trapping are also discussed.[34] The 2D quantum mechanical studies of the ER mechanism for the recombinative desorption of H atoms with a similar PES performed by Kratzer and Brenig[25] also support their conclusions. All of those results show significance of quantum mechanical effects in gas-surface reactive scattering. However these models can not account for the surface vibrational motion (phonon), which is quite significant in gas-surface energy transfer.

In alternative approach, the one-dimensional Generalized Langevin Equation(GLE) method, attempted for gas-surface reactive scattering by Ree, Kim and Shin,[8] surface modes are treated as a one-dimensional chain. They applied the MTGLE (Molecular Time-scale Generalized Langevin Equation). method[8-10,15] to O + H/W, O + CO/Pt and H + H/Si(100)-(2 × 1) reaction systems and calculated translational and vibrational energy distributions and the likely reaction mechanism. They demonstrate the significance of surface modes in energy transfer. The method is quite successful for understanding reaction mechanisms.

In the present paper, we have proposed a three-dimensional GLE approach to gas-surface reactive scattering model H + H → H_2/Si(100)-(2 × 1) system. The implementation of the 3D GLE method on hydrogen on silicon surface is presented. The frequencies of surface vibrations are calculated. The reaction probabilities are calculated for two energies. Very large amount of energy is transferred in surface in low energy scattering. The significant role of surface modes in energy transfer are discussed.

In Section II, a brief description of the implementation of the 3D GLE approach to gas-surface reactive scattering is presented. Numerical details of the scattering calculations and interaction potentials are described in Section III. Results and discussions are given in Section IV.

Implementation of 3D GLE to Gas-surface Reactive Scattering

The GLE approach was first applied to gas-surface collisions by Adelman and Doll,[26] based on the ideas of Zwanzig,[27] Mori,[28] and Kubo[29] for studying gas-surface diffusion dynamics. Tully and coworker[30-32] extended the method not only to gas-surface diffusion[30,31] but also to gas-surface inelastic scattering[32] and have shown it to be a powerful method when the surface modes play an important role. The details of approach to gas-surface interactions, especially for non reactive systems, are reported elsewhere,[32] and the 1D approach to reactive systems is reported by Ree, Kim and Shin.[8] We will present only the salient features of 3D GLE on a reactive scattering system.

The GLE approach to gas-surface reactive scattering has two basic assumptions. One is that the solid is harmonic. Thus, in the absence of gas molecules the motion of solid atoms satisfy the equation

$$\ddot{u}(t) = -\Omega^2 u(t), \tag{1}$$

where Ω is the matrix of force defined as

$$\Omega_{ij}^2 = (m_i m_j)^{-1/2} K_{ij}, \tag{2}$$

where m_i is the mass of atom i and K_{ij} is a force constant.

The other assumption is that the forces on the atoms in the molecule are determined by only a small number of local surface atoms named the primary zone. The remaining infinite number of surface and bulk atoms are designated as the secondary zone. We defined P and Q as projection operators, which select the primary zone and the secondary zone, respectively.

$$y(t) = \mathrm{P}u(t), \tag{3}$$

where $y(t)$ are the mass-weighted coordinates of the primary atoms.

$$z(t) = (1-P)u(t) = Qu(t), \tag{4}$$

where $z(t)$ are the mass-weighted coordinates of the secondary atoms.

In accordance with this definitions the classical equation of motion for gas-surface reactive scattering systems can be written as

$$\ddot{x}(t) = F_R[x(t), y(t), z^0] \tag{5}$$

$$\ddot{y}(t) = -\Omega_P^2 y(t) - \Omega_{PQ}^2 z(t) + F_P[x(t), y(t), z^0] \tag{6}$$

$$\ddot{z}(t) = -\Omega_{QP}^2 y(t) - \Omega_Q^2 z(t), \tag{7}$$

where

$$\begin{aligned} \Omega_P^2 &= P\Omega^2 P \\ \Omega_Q^2 &= Q\Omega^2 Q \\ \Omega_{QP}^2 &= Q\Omega^2 P \\ \Omega_{PQ}^2 &= P\Omega^2 Q \end{aligned} \tag{8}$$

and $x(t)$ are the mass-weighted coordinates of the gas atoms in the molecule. F_R and F_P are mass-weighted forces derived from the gas-surface interaction potential V by

$$\begin{aligned} F_{R_i}[x(t), y(t), z^0] &= -\partial V[x(t), y(t), z^0]/\partial x_i \\ F_{P_i}[x(t), y(t), z^0] &= -\partial V[x(t), y(t), z^0]/\partial y_i \end{aligned} \tag{9}$$

and the forces can depend on the equilibrium positions z^0 of the secondary lattice atoms.

Eq. (7) can be solved formally by Laplace transformation and substituted into Eq. (6) to yield the GLE

$$\ddot{y}(t) = -\Omega_{eff}^2 y(t) - \Lambda(t) y(0) - \int_0^t \Lambda(t-t')\dot{y}(t')dt' + R(t) + F_P[x(t), y(t), z^0], \tag{10}$$

where

$$\Omega_{eff}^2 = \Omega_P^2 - \Lambda(0) \tag{11}$$

$$\Lambda(t) = \Omega_{PQ}^2 \cos[\Omega_Q t]\Omega_Q^{-2}\Omega_{QP}^2 \tag{12}$$

$$R(t) = -\Omega_{PQ}^2 \cos[\Omega_Q t] z(0) - \Omega_{PQ}^2 \Omega_Q^{-1} \sin[\Omega_Q t]\dot{z}(0) \tag{13}$$

Thus, we have accomplished an exact replacement of the infinite set of coupled equations, Eqs. (5)-(7), by the small number of equations, Eqs. (5) and (10).

The GLE's, Eq. (10), are exact, but the friction kernel $\Lambda(t)$ and fluctuating force $R(t)$ are very complicated. Tully has shown that the friction kernel (t) can be approximated by the multi-dimensional generalization of a position autocorrelation of a Brownian harmonic oscillator,

$$\Lambda(t) = \Lambda_0 \exp\left(-\frac{1}{2}\gamma t\right)\left[\cos(\omega_1 t) + \frac{1}{2}\omega_1^{-1}\sin(\omega_1 t)\right], \tag{14}$$

where Λ_0, γ, and ω_1, are commuting matrices. Then, Eq. (10) becomes

$$\ddot{y}(t) = -\Omega_P^2 y(t) + \Lambda_0^{1/2}\omega_0 s(t) + F_P[x(t), y(t), z^0] \tag{15}$$

$$\dot{s}(t) = -\Lambda_0^{1/2}\omega_0 y(t) - \omega_0^2 s(t) - \gamma\dot{s}(t) + \xi(t), \tag{16}$$

where

$$\omega_0^2 = \omega_1^2 + \gamma^2/4, \tag{17}$$

and (t) is a white-noise Gaussian random force satisfying

$$\langle \xi(0)\xi^+(t)\rangle = 2k_B T\gamma\delta(t). \tag{18}$$

The effective particles $s(t)$ do not correspond to any particular secondary lattice atoms. They describe the net energy flow between the primary and secondary zones and, thus, can be thought to represent the response of a local region of the lattice. A similar use of "ghost particles" was employed elsewhere.[30,31] In our work, some modifications were made to allow the treatment of surfaces that have various properties such as optical modes, defects, steps, and also to allow the study of processes that involve reactions with surface atoms, including sputtering and chemical etching.

We have chosen a primary zone containing 28 atoms to represent the Si(100) surface. Rather than attaching addi-

tional ghost atoms to the surface, we have chosen to attach simple friction and random forces identical in form to those attached to the ghost atoms to the atoms on the edges of the primary lattice zone. These forces also obey the fluctuation-dissipation theorem so that a well defined temperature T can be established in the primary zone. Also additional forces must be added to the boundary degree of freedom, which represent forces between primary and secondary atoms equivalent to the ω_0^2 forces. The equation of motion for the primary lattice atoms is then

$$\ddot{y}(t) = -\Omega_{eff}^2 y(t) - \gamma\dot{y}(t) + \xi(t) + F_P[x(t), y(t), z^0] \quad (19)$$

where some elements of the vectors γ and $\xi(t)$ are zero, depending on the position of the corresponding atom the primary zone.

Potential Energy Surface and Calculations

The model Si(100)-(2 × 1) harmonic slab is given previously by Lucchese and Tully.[20] The harmonic slab consists of 28 Si atoms for the primary zone and 85 Si atoms for the secondary zone. The primary zone has 16 atoms for the first layer and 12 atoms for the second layer. The secondary zone is formed with 32 atoms in the first plane, 28 atoms in the second plane and 25 atoms in the third plane. We did not account for continuum contribution under the third layer. The harmonic interaction between the Si atoms includes the bond stretching force between nearest neighbors, K_R, with the force constant of 1.469 mdyn/Å^3 and a harmonic force between second nearest neighbors with a force constant of 0.0890 mdyn/Å^3, which is a two-body approximation to the bending mode, H_A. In representing the Si(100)-(2 × 1) surface, we kept the 12 atoms in the second plane of the surface in positions identical to the bulk structure, and we formed surface dimers with the 16 atoms in the first plane, with the dimer geometries corresponding to the singlet geometry predicted by Redondo and Goddard.[33] Thus the surface dimer bond length is 2.47 Å and the bond length between atoms in the first plane and second plane is 2.37 Å.

The interaction potential between adsorbed H, impinging H and Si atoms in the primary zone is LEPS type pairwise sum of Morse potential for the system. The reaction system H-H-Si is treated with LEPS potential, whereas all the other H-Si pairs are Morse potential. The LEPS potential is given as follows.

$$E_{total} = V_{HH} + V_{SiH_1} + V_{SiH_2} - A_{total} \quad (20)$$

$$A_{total} = \sqrt{A_{HH}^2 + A_{SiH_1}^2 + A_{SiH_2}^2 - A_{HH}(A_{SiH_1} + A_{SiH_2}) - A_{SiH_1}A_{SiH_2}} \quad (21)$$

$$V_i = \frac{D_i}{4(1+\Delta_i)}[(3+\Delta_i)\exp(-2\alpha_i(r_i - r_{0i})) - (2+6\Delta_i)\exp(-\alpha_i(r_i - r_{0i}))] \quad (22)$$

$$-(6+2\Delta_i)\exp(-\alpha_i(r_i - r_{0i}))], \quad (23)$$

where i=H_1H_2, SiH_1, SiH_2. The parameters are given in Table 1.

Table 1. Potental parameters for H + H → H_2/Si(100)-(2 × 1) system

	De (eV)	α (Å^{-1})	R_e (Å)	Δ (Sato parameter)
H_1-H_2[a]	4.75	1.943	0.74	0.10
Si-H_1[b]	3.45	1.512	1.51	0.12
Si-H_2[c]	3.45	1.512	1.51	0.11

[a]Data from reference 34. [b,c]Data from reference 35.

The classical trajectory calculations were performed in the usual manner. The incident kinetic energy is fixed at a particular value corresponding to a monoenergetic molecular beam and incidence normal to the surface is assumed in all calculations. Target sites were sampled at even spacing within the impact area. The initial positions and momenta of the solid atoms were chosen randomly from a thermal statistical canonical ensemble for a given temperature. Hamilton's equations of motion were solved numerically by a variable-order, variable-step method implementing the Backward Differentiation Formulae (BDF).

Results and Discussion

We performed three different kinds of calculations to test whether this 3D GLE formalism and algorithm on the reactive scattering work properly. First, we calculated the 84 normal mode frequencies and eigenvectors for the primary zone of the reconstructed Si(100)-(2 × 1) solid. Table 2 gives the normal mode frequencies. The frequencies are almost identical compared with previous harmonic slab calculations on

Table 2. The normal mode frequencies for the Si(100)-(2 × 1) reconstructed surface

No.	ω (cm^{-1})	No.	ω (cm^{-1})	No.	ω (cm^{-1})	No.	ω (cm^{-1})
1	123.85	22	224.24	43	423.38	64	500.15
2	123.85	23	242.93	44	423.54	65	502.06
3	123.85	24	243.20	45	439.78	66	502.11
4	123.90	25	247.76	46	441.06	67	503.76
5	127.46	26	250.10	47	445.68	68	503.81
6	127.46	27	263.63	48	446.79	69	506.41
7	127.46	28	265.17	49	460.75	70	506.46
8	127.51	29	277.23	50	464.20	71	507.31
9	138.50	30	277.49	51	464.47	72	508.11
10	138.56	31	287.63	52	464.58	73	538.85
11	139.57	32	288.21	53	465.48	74	543.62
12	140.20	33	361.90	54	468.08	75	545.75
13	151.46	34	363.76	55	469.83	76	550.00
14	151.46	35	365.83	56	473.49	77	550.00
15	154.48	36	367.48	57	480.34	78	552.12
16	155.07	37	398.96	58	481.51	79	554.24
17	155.12	38	401.35	59	498.71	80	554.77
18	157.24	39	410.05	60	499.03	81	555.84
19	160.27	40	412.34	61	499.40	82	557.96
20	163.93	41	422.48	62	499.77	83	559.02
21	224.03	42	422.69	63	500.04	84	561.14

Table 3. Eenergy transfer to solid

Incident Energy (eV)	Final Energy (eV)	Ratio
0.00	0 (adsorbed)	1.00
0.02	0 (adrorbed)	1.00
0.04	0 (adsorbed)	1.00
0.05	3.51×10^{-3}	0.93
0.06	6.68×10^{-3}	0.89
0.08	2.57×10^{-2}	0.68
0.10	4.44×10^{-2}	0.56
0.12	6.27×10^{-2}	0.47
0.14	8.10×10^{-2}	0.42

Si(100)-(2 × 1) surface by Park and Bowman.[17] This implies the lattice of 3D GLE does work properly.

Second, before going to the H + H → H_2/Si(100)-(2 × 1) reaction, we tested the adsorption and desorption of H atom on the surface. Hydrogen atoms are impinged to the target site from 0 eV to 0.14 eV. Table 3 shows kinetic energy transfer to the solid as a function of incident kinetic energy. When the incident kinetic energy is less than 0.05 eV, all of the hydrogen atoms are adsorbed on the surface. The ratio of energy transfer to the surface decreases with increasing incident kinetic energy. Using these trajectories one can extract information on adsorption sites dynamically. For the monohydrided Si surface, the most stable site for the adsorbed H atom is almost on top of the Si atom.[14] H is bonded to a Si atom of the Si dimer with a bond length of 1.51 Å, forming a bond angle of 112.3° with the Si-Si dimer bond. When a single H atom is adsorbed, the information on the stable adsorption site was unavailable due to experimental difficulties. We do not have any information on the adsorption site of the H atom in the H + H → H_2/Si(100)-(2 × 1) reaction. This calculation gives the results on the adsorption site of the H atom. Figure. shows the motion of a typical trajectory of an adsorbed H atom. As shown in Figure 1, H atoms vibrate on the surface around a specific point. The average value of the trajectories is (4.01, 1.92, 1.00) in Å unit. We used this value as a stable adsorption site in the remaining calculation of the H + H → H_2/Si(100)-(2 × 1) reaction.

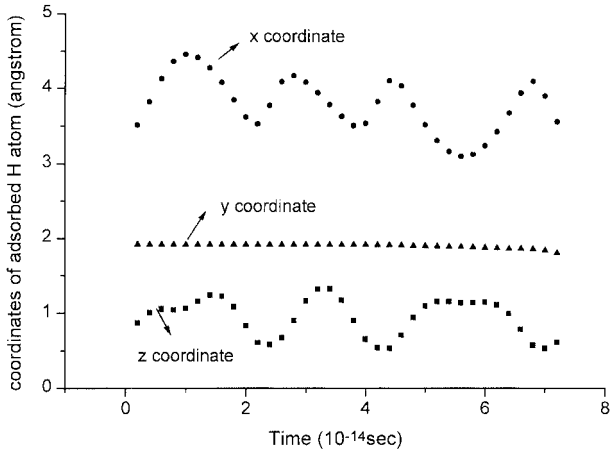

Figure 1. Coordinates of adsorbed H atom as a function of time.

Table 4. Reaction Probabilities

Incident energy (eV)	b_{max} (Å)	Product as H_2	Adsobed as H	Adsorbed as H_2
0.06	1.41	0.19	0.58	0.23
0.06	3.95	0.14	0.73	0.13

Since our interest is focused on whether the 3D GLE formalism and algorithm working on the reactive scattering system, we did not calculate vibrational rotational energy distributions in the present work. 1000 trajectories are propagated onto the surface for given the kinetic energy of 0.06 eV. Reaction probabilities and adsorption probabilities are given in Table 4. The reaction probabilities are 0.19 and 0.14, respectively, for the given maximum impact parameters, 1.41 Å and 3.95 Å. The reaction probabilities are lower than for the rigid surface model by Kratzer[14] but qualitatively close to 1D GLE model by Lim *et al.*[15] As is easily expected, the transition probability of the rigid model is fairy over estimated, because the model can not have energy exchanged to the surface due to the rigid nature of the solid. Large portions of the trajectories, more than 50 percent, are adsorbed on solid as atomic hydrogen. For the collision energy of 0.06 eV and the maximum impact parameter of 1.41 Å, 58 percent of the trajectories do not formed molecular hydrogen at all, and 42 percent of the trajectories formed molecular hydrogen. Among them 19 percent of the trajectories gave H_2 molecules that could escape from the surface. 23 percent of the trajectories were formed as molecular hydrogen that could not escape from the surface. The molecular hydrogens were either diffused or migrated on the surface. When the maximum impact parameter was increased to 3.95 Å, reaction probability was decreased to 0.14. 73 percent of the H atoms were either adsorbed on the surface or penetrated into the solid. Only 27 percent of the trajectories formed molecular hydrogen. Among them, 14 percent gave H_2 molecules that escaped from the surface. 13 percent of the trajectories were formed as molecular hydrogen that could not escape the surface. They were either diffused or migrated on the surface. As the silicon solid has a rather loose nature, this is quite reasonable.

In order to understand this phenomena, we analyzed typical reactive, nonreactive and diffusive trajectories. Figure 2a and Figure 2b show a typical reactive trajectory. When the incident kinetic energy is larger than the threshold energy (0.05 eV), reaction can occur and molecular hydrogen can have enough energy to escape from the surface. As shown in Figure 2a, the distance between the impinging H atom (denoted as 1) and the adsorbed H atom (denoted as 2) decreases, and molecular hydrogen is formed. The distance between the adsorbed H atom and the silicon atom start vibrating and increasing to more than 5 Å, which indicates escape from the surface. Figure 2b shows the z-coordinate of the impinging H atom and the adsorbed H atom. The z-coordinate of atom H_1 decreases and then increases after the molecule is formed, whereas the z-coordinate of the atom H_2 is vibrating and then increases. The two figures support each

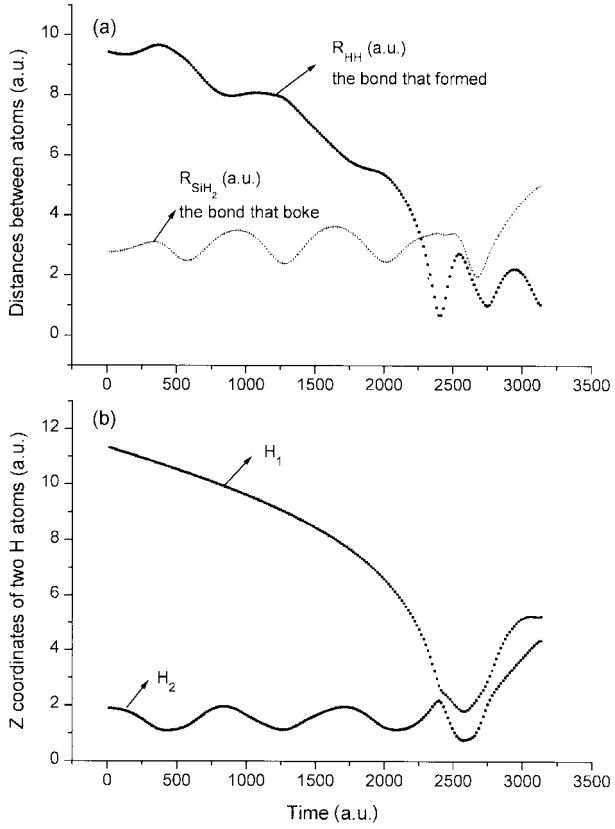

Figure 2. (a) Distance between atoms. The symbols, (●) and (+) indicate $R_{H\text{-}H}$ and $R_{Si\text{-}H}$ respectively. (b) The z-coordinates of the impinging H atom and the adsorbed H atom H. The symbols, (■) and (●) indicate the impinging H atom and the adsorbed H atom respectively which is denoted as H_1 and H_2.

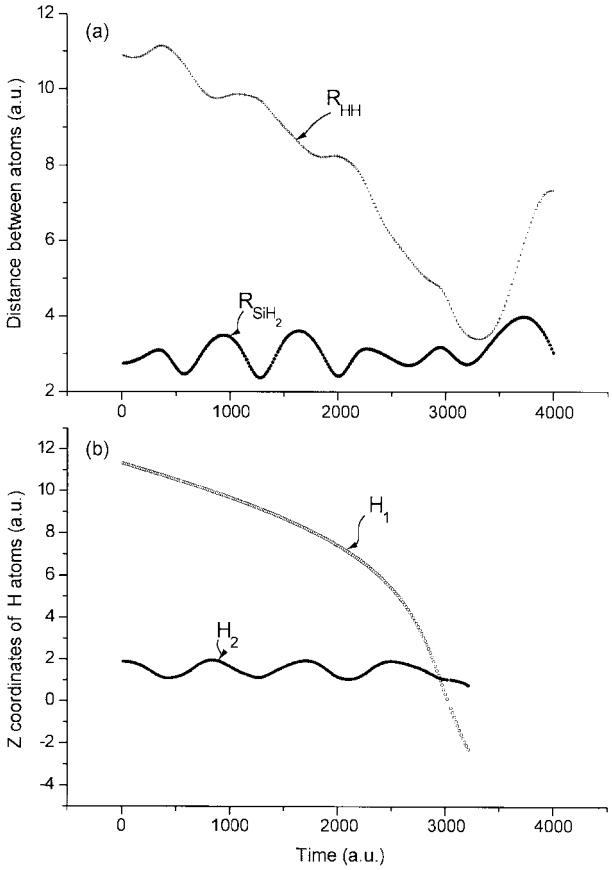

Figure 3. (a) Distance between atoms. The symbols, (+) and (◆) indicate $R_{H\text{-}H}$ and $R_{Si\text{-}H}$ respectively. (b) The z-coordinates of the impinging H atom and the adsorbed H atom H. The symbols, (○) and (●) indicate the impinging H atom and the adsorbed H atom respectively which is denoted as H_1 and H_2.

other.

Figure 3a and Figure 3b show non the reactive nature of a typical trajectory, where the initial condition of the impact parameter is 3.95 Å. As shown in Figure 3a, the distance between the impinging H atom and the adsorbed H atom decreases and increases, and they do not form molecular hydrogen. The distance between the adsorbed H atom and the silicon atom start vibrating, but is not altered much by the incident H atom. Figure 3b shows the z-coordinate of the impinging H atom and the adsorbed H atom. The z-coordinate of atom H_1 decreases and penetrates to the first layer, the z-coordinate of atom H_2 does not change. These figures support the non reactive nature of the trajectory.

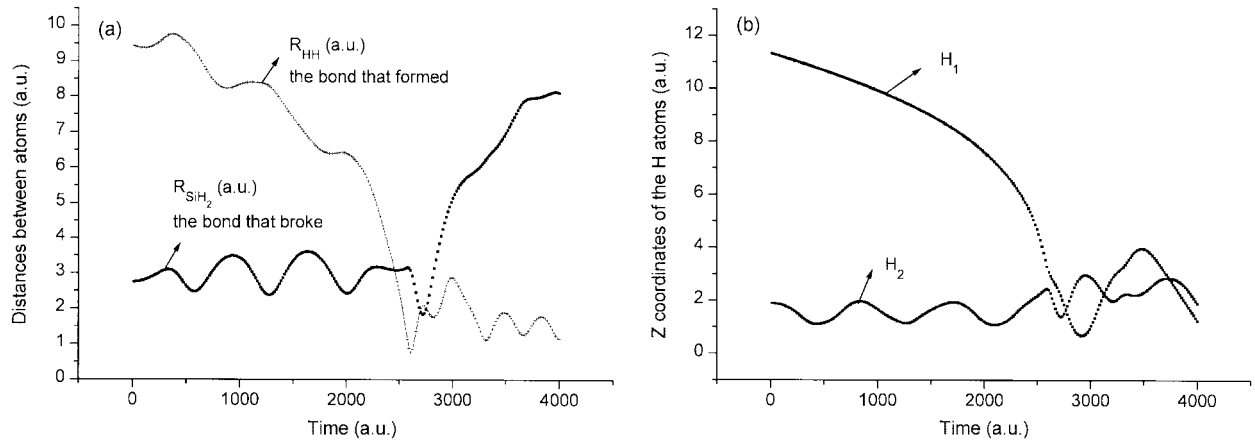

Figure 4. (a) Distance between atoms. The symbols, (+) and (●) indicate $R_{H\text{-}H}$ and $R_{Si\text{-}H}$ respectively. (b) The z-coordinates of the impinging H atom and the adsorbed H atom H. The symbols, (■) and (■) indicate the impinging H atom and the adsorbed H atom respectively which is denoted as H_1 and H_2.

The third type of reaction forms molecular hydrogen, but the molecular hydrogen does not have enough z-component energy to escape from the surface. Figure 4a and 4b show the diffusive nature of the reactive trajectory. As shown in the Figure 4a, the distance between the impinging H atom and the adsorbed H atom decreases and molecular hydrogen is formed. The distance between the adsorbed H atom and the silicon atom start vibrating and changes vibration pattern. This shows that the molecular hydrogen is intact on the silicon atom and stays on the surface. Figure 4b supports the intact nature of the molecular hydrogen. The z-coordinate of the impinging H atom and the adsorbed H atom show the formation of molecular hydrogen. The z-coordinate of atom H_1 decreases and fluctuates when the bond is formed. It does not increase any further which indicate the atom can not escape from the surface. The z-coordinate of atom H_2 shows vibration and fluctuation which also indicate the atom can not escape from the surface.

Summary

In tyhe present study, we propose a three-dimensional GLE approach to gas-surface reactive scattering model H + H $\rightarrow$ H_2/Si(100)-(2 $\times$ 1) system. The implementation of the 3D GLE method on the hydrogen on silicon surface is presented. The formalism and algorithm of the 3D GLE worked properly in the reactive scattering system. The calculated normal mode frequencies of the surface vibrations are almost identical to previous harmonic slab calculationsw. The reaction probabilities are calculated for two energies. A very large amount of energy is transferred in surface in low energy scattering. Three different types of reaction mechanisms have shown which can not be represented in flat and rigid surface models. More details of the reaction mechanisms and calculations of vibrational and rotation distributions of products are in progress. These will be reported soon elsewhere.

Acknowledgment. The authors wish to acknowledge the financial support of the Korea Research Foundation made in the program year of 1997. Y. Zhang acknowledges the binational program between Sungkyunkwan University of Korea and Shandong University of China.

References

1. *Dynamics of Gas-Surface Interactions*; Rettner, C. T., Ashfold, M. N., Eds.; Royal Society of London: Thomas Graham House, Cambridge, 1991.
2. Somorjai, G. A. *Introduction to Surface Chemistry and Catalysis*; Wiley: New York, 1991.
3. Mogab, C. J. In *VLSI Technology*; Sze, S. M., Ed.; McGraw-Hill: New York, 1983; Chapter 8, pp 303-346.
4. Rettner, C. T.; Auerbach, D. J. *Science* **1994**, *263*, 365.
5. Rettner, C. T. *J. Chem. Phys.* **1994**, *101*, 1529.
6. Park, S. C.; Bowman, J. M.; Jelski, D. *J. Chem. Phys.* **1996**, *104*, 2457.
7. Park, S. C.; Park, W. K.; Bowman, J. M. *Surf. Sci.* **1999**, *427*, 343.
8. Ree, J.; Kim, Y. H.; Shin, H. K. *J. Chem. Phys.* **1996**, *104*, 742.
9. Ree, J.; Kim, Y. H.; Shin, H. K. *J. Phys. Chem. A* **1997**, *101*, 4523.
10. Kim, Y. H.; Ree, J.; Shin, H. K. *J. Chem. Phys.* **1998**, *108*, 9821.
11. Sheng, J.; Zhang, J. Z. *J. Chem. Phys.* **1992**, *96*, 3866.
12. Sheng, J.; Zhang, J. Z. *J. Chem. Phys.* **1992**, *96*, 3866.
13. Brau, P.; Brenig, W.; Kratzer, P.; Russ, R. *Phys. Rev. B* **1996**, *54*, 5978.
14. Kratzer, P. *J. Chem. Phys*. **1997**, *106*, 6752.
15. Lim, S.-H.; Ree, J.; Kim, Y. H. *Bull. Korean Chem. Soc.* **1999**, *20*, 1136.
16. Park S. C.; Clary, D. C. *J. Appl. Phys.* **1986**, *60*, 1183.
17. Park, S. C.; Bowman, J. M. *J. Chem. Phys.* **1984**, *81*, 6277.
18. Park, S. C.; Bowman, J. M. *Chem. Phys. Lett.* **1985**, *119*, 275.
19. Park, S. C.; Rhee, C. H.; Hwang, W. L.; Lee, Y. S.; Kim, M. S. *Bull. Korean Chem. Soc.* **1991**, *12*, 387.
20. Lucchese, R. R.; Tully, J. C. *Surf. Sci.* **1983**, *137*, 570.
21. Jackson, B.; Persson, M. *Surf. Sci*. **1992**, *269/270*, 195.
22. Jackson, B.; Persson, M. *J. Chem. Phys.* **1992**, *96*, 2378.
23. Persson, M.; Jackson, B. *J. Chem. Phys.* **1995**, *102*, 1078.
24. Jackson, B.; Persson, M. *J. Chem. Phys.* **1995**, *103*, 6257.
25. Kratzer, P.; Brenig, W. *Surf. Sci.* **1991**, *254*, 275.
26. Adelman, S. A.; Doll, J. D. *J. Chem. Phys.* **1974**, *61*, 4242.
27. Zwanzig, R. *J. Chem. Phys.* **1960**, *32*, 1173.
28. Mori, H. *Prog. Theor. Phys.* **1965**, *33*, 423.
29. Kubo, R. *Rep. Prog. Theor. Phys.* **1966**, *29*, 255.
30. Shugard, M.; Tully, J. C.; Nitzan, A. *J. Chem. Phys.* **1977**, *66*, 2534.
31. Tully, J. C. *J. Chem. Phys.* **1980**, *73*, 1975.
32. Lucchese, R. R.; Tully, J. C. *J. Chem. Phys.* **1984**, *80*, 3451.
33. Redondo, A.; Goddard III, W. A.; Vacuum, J. *Sci. Technol.* **1982**, *21*, 344.
34. Huber, K. P.; Herzberg, G. *Constants of Diatomic Molecules*; Van Nostrand: Reinhold, New York, 1979.
35. Wu, C. J.; Carter, E. A. *Chem. Phys. Lett.* **1991**, *185*, 172.